Probability of defect propagation in pipelines (POP curves)

C F C Pinto, R R da Silva, L P Calôba and S D Soares

Submitted 27.10.13
Accepted 02.03.14

Monitoring equipment in real time has become increasingly important, mainly when operational safety is targeted. Acoustic emission (AE) testing has been applied to the inspection of various types of equipment, particularly rigid pipes. This paper presents a study on the use of acoustic emission to detect defect propagation in pressurised rigid pipes. The resulting AE signals were classified as no propagation (NP), stable propagation (SP) and unstable propagation (UP) and used as inputs in the implementation of non-linear classifiers by error back-propagation. The correct classification results reached close to 91%, proving the efficiency of the method in the conditions tested in this study. The methodologies used for the construction of the probability of propagation (POP) curve are presented, which are a great innovation in this research field and the focus of an international patent.

Keywords: non-destructive testing (NDT), acoustic emission, non-linear pattern classifiers, neural network.

Carlos Fernando Carlim Pinto graduated in electronic and computer engineering from the Federal University of Rio de Janeiro (UFRJ) in 2009 and attained his master's degree in electrical engineering from UFRJ in 2011. He is presently a DSc student in electrical engineering in the Signal Processing Laboratory, Federal University of Rio de Janeiro, Rio de Janeiro, Brazil, and works on research projects related to pattern recognition and neural networks. Email: carlos.fernando@lps.ufrj.br

Romeu Ricardo da Silva graduated in metallurgical engineering from the Federal University of Rio de Janeiro (UFRJ) in 1997, attained his master's degree in material and metallurgical engineering from UFRJ in 1999 and his DSc degree in material and metallurgical engineering from UFRJ in 2003, with a post-doctorate from the Universidad Católica de Chile in 2007. He is presently a technical consultant of projects with COPPE, Signal Processing Laboratory, Federal University of Rio de Janeiro, Rio de Janeiro, Brazil. Email: romeu@romeu.eng.br

Luiz Pereira Calôba graduated in electronic engineering from the Federal University of Rio de Janeiro (UFRJ) in 1969, attained his master's degree in electrical engineering from UFRJ in 1970 and a Dr Ing degree from the Université Scientifique et Médicale de Grenoble in 1974. He is presently Professor (Emeritus) in the Signal Processing Laboratory, Federal University of Rio de Janeiro, Rio de Janeiro, Brazil. His areas of interest are neural networks and signal processing. Email: caloba@lps.ufrj.br

Sergio Damasceno Soares graduated in mechanical engineering from the Faculdade de Engenharia Souza Marques in 1991, attained his master's degree in metallurgical and materials engineering from UFRJ in 1998 and his DSc degree in metallurgical and materials engineering from UFRJ in 2008. He is presently an engineer with the Research Center Leopoldo Américo Miguez de Mello (CENPES/PETROBRAS), Petrobras, Rio de Janeiro, Brazil. He has experience in the area of materials and metallurgical engineering, with an emphasis on non-destructive testing. Email: sdama@petrobras.com.br

Introduction

In the modern world, the use of non-destructive testing (NDT) to assess the structural integrity of equipment is of undeniable importance. In the past, tests were basically restricted to visual testing, liquid penetrant, magnetic particle, radiography and ultrasound. Among current NDT, the method of acoustic emission (AE) is based on the detection of sources of acoustic signals that are emitted during the propagation of discontinuities and sharp plastic deformation. As it is a qualitative method, the AE test does not provide the dimensions of the discontinuities, which are provided by other NDT methods such as ultrasound. Since it only provides indications of active discontinuities during the loading of structures, one of the main goals of its application is real-time monitoring of equipment.

Motivated by the importance of acoustic emission for non-destructive inspection of equipment, and the capability of implementing non-linear classifiers by neural network techniques, this paper describes a study developed to implement non-linear pattern classifiers, aiming to detect the growth of defects in rigid pipes using the parameters of AE signals as the input set[1]. The signals were divided into three classes: no propagation, stable propagation and unstable propagation, defined by ultrasound monitoring of growth defects, synchronised with hydrostatic testing[2].

The results of the development of the classification probability techniques supply the foundation for the construction of probability of propagation (POP) curves, which have a similar shape to the well-known probability of detection (POD) curves; however, they are conceptually different. In this way, we present the concept of the formation of POP curves and the first results obtained, which will guide future studies.

2. Analysis of acoustic emission tests

2.1 Materials

The specimens were made of API XL Grade 60 steel, 20 inches in diameter and 14.5 mm in thickness. An elliptical crack localised exactly on the TOFD transducer (Figure 1) was machined on the inner and outer surfaces of the pipes, with different dimensions for each test. For illustration, Figure 1 contains a typical schematic drawing of a pipe section with the instrumentation used for monitoring by hydrostatic tests.

The crack on the inner surface of the specimen was machined with a grinder using a cutting disc with a radius of 12 mm. The defect had a semi-elliptical shape 160 mm long, 1.1 mm wide and 7.33 mm deep.

2.2 Acquisition parameters of acoustic emission

Acoustic emission signals were acquired during the hydrostatic pressure tests, using the Disp 16 c equipment of PASA (Physical Acoustics South America). Eight sensors were used: four near the crack and two located at each o-ring. After the acquisition, the signals were processed in the same equipment.

According to Pinto[2], the correct classification of AE signals into one of the three proposed classes requires nineteen features, which are described in Table 1.

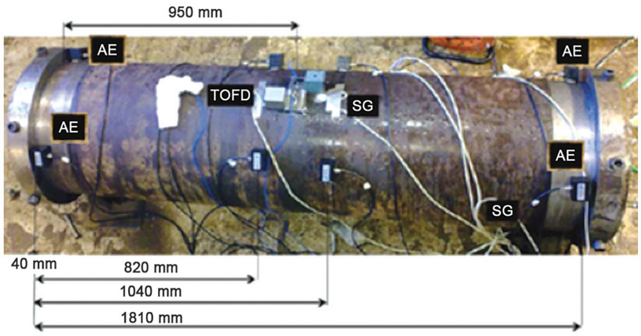

Figure 1. Schematic of positioning of the sensors close to the region of the crack on the inner surface of the specimens. Dimensions in mm. TOFD: ultrasound transducer; SG: strain gauge sensor; AE: acoustic emission sensor

Table 1. Acoustic emission features collected[2]

Feature	Description
Rise	Time interval between the first peak that exceeds the reference threshold and the maximum peak amplitude.
Count	Number of times the signal exceeds the threshold, within the value set of HDT.
Energy	Integral of absolute value of each wave peak. Since this is a discrete time signal, sum up the values of the samples of rectified waveform. It must be pointed out that breadth here refers to a measure of voltage and not decibel.
Duration	Time interval between the first and the last thresholds exceeded within the pre-set value of HDT.
AMP	Maximum peak amplitude of the signal, in dB.
A-Freq	Average frequency: the definition is count over duration (count/duration).
RMS	The root of the integral values of voltage squared divided by the interval given by the time difference between the upper and lower limits of integration.
ASL	Average signal level, in dB.
PCNTS	Number of peaks until the maximum amplitude is reached, always taking into account the reference threshold.
R-Freq	Reverb frequency: defined by (count-count to peak)/(duration-rise time).
I-Freq	Initiation frequency: defined by (count to peak / rise time).
Sig-Strength	Signal strength or intensity: practically the definition of power, but with simpler coefficient of sen (π/4).
ABS-Energy	This is a normalised parameter that represents the real amount of energy in pico-joule. It is defined by the sum of the amplitudes of samples squared divided by 10 (kOhm impedance).
Freq-PP1	First partial power.
Freq-PP2	Second partial power.
Freq-PP3	Third partial power.
Freq-PP4	Fourth partial power.
C-Freq	Centroid frequency: not necessarily the centre frequency, corresponding to the centre of the spectrum, but choosing a setting that takes into account 'weights' due to the magnitude and spraying.
P-Freq	Peak frequency: frequency component of greater magnitude in the spectrum.

2.3 Synchronisation of files of acoustic emission signals

Since the monitoring of pressurisation and growth of artificial defects and the acoustic emission signals are always in separate files, a procedure for synchronising them was established, because the acoustic emission activity is related to the load and to the propagation of the defect. The AE signals resulting from tests were filtered to separate, by arrival time, just those that provided the sensors close to defects.

2.4 Separation of signals

After synchronising the files, the acoustic emission events were divided into the following classes: no propagation (NP), stable propagation (SP) and unstable propagation (UP)[2].

2.5 The neural classifier

Artificial neural networks were used to implement non-linear pattern classifiers[3,4].

The classifiers were developed using the back-propagation algorithm, a multilayer feed forward topology and performed as the hyperbolic tangent activation function. Some configurations of training parameters were studied to provide the best possible classification and to ensure the generalisation of classifiers[3,4]. Several datasets for training and testing were randomly selected without data replacement, aiming to estimate the accuracy of the identification signals of no propagation (NP), stable propagation (SP) and unstable propagation (UP) of defects, as well as two classes (NP and P).

After training had been conducted several times to assess which would be the best classifier configuration to be used with the inputs provided, aiming at the best possible generalisation (testing for three classes), we defined a good classifier with six neurons in the hidden layer and a momentum of 0.9, a variable learning rate with an initial value at 0.05, a growth factor of 1.05 and a decrease factor of 0.9, and set the maximum at 0.2 (parameters adjusted in the Matlab program). Once the best parameters to be used in network training were set, we decided to test them using a random selection without replacing the sets of training (80%) and test (20%)[5]. More details can be obtained in Silva *et al*[6].

3. Probability of propagation (POP) curve

The main objective of the POP curve is to use the output values of each neuron of the classifier output layer for calculation of the probability of classification. To determine the probability, only two sets of data are relevant: the one that belongs to the class and the one that does not belong to the chosen class.

Figure 2 can be analysed in order to explain the methodology defining the NP class as stage 1 in propagation, SP as stage 2 and UP as stage 3, assuming that the probability in relation to time for the NP class is near 1, while the others are close to zero at the threshold of the definition of this class. When entering the second stage, the SP class probability should be close to one and the remainder close to zero. In the third and last stage, the probability of the UP class should be close to one and the remainder to zero. When plotting the three probabilities in one single graphic in relation to time, the probability of propagation (POP) curve is generated.

In an ideal situation, we assume that the AE testing for crack propagation monitoring in a pressurised equipment lasted 150 s, being that the signals of the first 49 s were defined as NP, from 50 s to 99 s as SP and from 100 s to 150 s as UP. Observing the graphic in Figure 3: from 0 s to 49 s, the probability of the signal being NP is equal to one, while the remainder is equal to zero; between 51 s and 99 s, the probability for SP is equal to 1 and the remainder is equal to zero; and from 100 s until the end of the testing, the probability for UP is equal to one and the remainder is equal to zero. However, it is highlighted that this would happen for an ideal signal characterisation situation, that is with 100% hit for

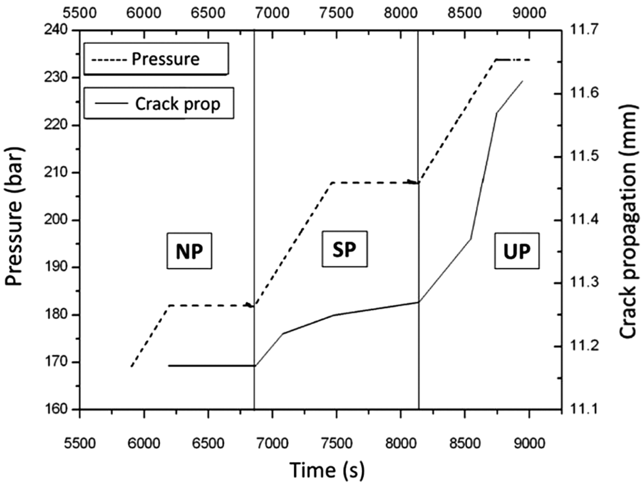

Figure 2. The dashed line represents the plot of pressure *versus* time and the continuous line represents the plot of crack propagation *versus* time

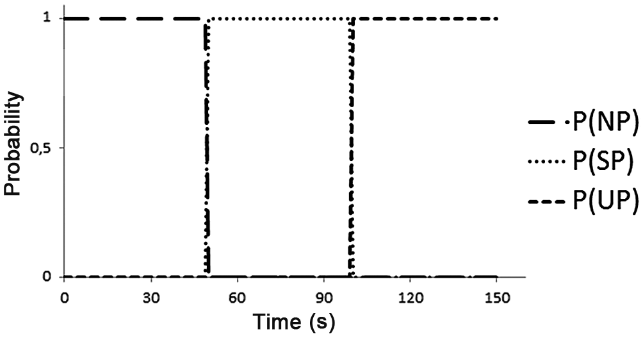

Figure 3. The long-dashed line represents the NP probability, the dotted line the SP probability and the short-dashed line the UP probability

the signals of each class in the defined region.

The testing time was used as a reference because, when there is a crack and the AE signal is captured, the tendency is for the propagation to occur until there is a rupture of the pipe, unless the pressure is relieved until the SP class. That is, in a t_{n+1} time, the size of the crack will be bigger or equal to the size in t_n, but never smaller.

This new approach can be characterised as a problem of recognition of statistical patterns, where the challenge lies in estimating the density functions in an n-dimensional space and dividing this space into classes[7].

In this new context, among the many classifiers Bayes classifiers are considered to be the best, since they minimise the error probability in classification. In the first classification stage, the non-parametric probability density function is estimated, since the data distribution is completely unknown[7]. In the second and last stage, the classification is done using Bayes theorem[8].

According to the neural network used to train the classifier, the classes were determined from the output value Y. Table 2 presents the values for each class.

Table 2. Neural network definitions

Class	Output vector Y
NP	$[1\ -1\ -1]^T$
SP	$[-1\ 1\ -1]^T$
UP	$[-1\ -1\ 1]^T$

According to Specht[9], the similarity between the feed-forward neural networks and non-parametric pattern classifiers is noticeable. The author affirms that this similarity can be observed in probabilistic neural networks, where the hyperbolic tangent activation function is replaced by an exponential function, the same as that used in the Gaussian kernel. Even though we are not developing a probabilistic neural network, we concluded that for the estimation of the probability distribution it is necessary that the activation function of each neuron of the output layer is removed according to Equation (1):

$$U_n = \tanh^{-1}(Y_n) \quad \text{.................................(1)}$$

so that n is the neuron and Y is the neuron's output.

After eliminating the activation function, the next step is to estimate the probability densities. The non-parametric probability functions are extremely difficult to precisely estimate compared to the parametric ones. However, the objective is not the precision of the estimated function but to use the curve to model the classifier[7,8].

Among the many methods for non-parametric estimation Parzen's stands out, which, when adjusted with a Gaussian kernel function K(.) so that $\int K(X)dX = 1$[7,8], can be interpreted as a weighted sum of the value of the K(.) function for each X value, as shown in Figure 4[10].

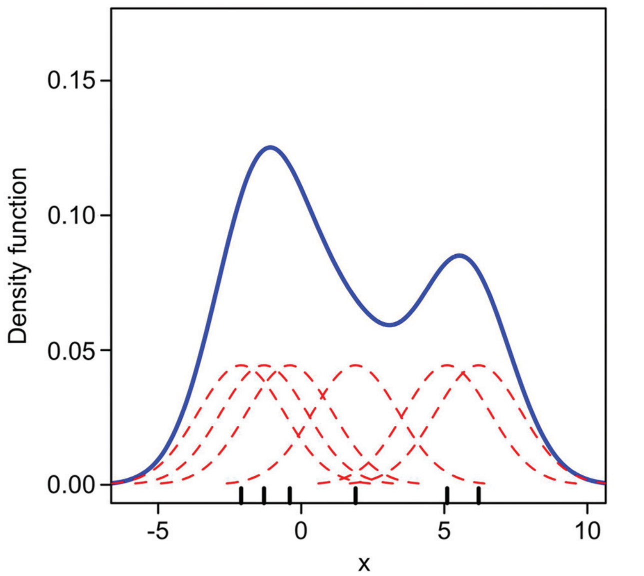

Figure 4. The curve with the continuous line is the estimated density and the dashed lines are the Kernel functions for each indicated point[10]

After estimating the probability density functions, the classification can be carried out using Bayes theorem, which will determine the *a posteriori* probability according to Equation (2)[8]. That is, given an input X, the probability of it belonging to the class is calculated:

$$\widehat{Pr}\left(G = j \middle| X = x_0\right) = \frac{\hat{\pi}_j \hat{f}_j(x_0)}{\sum_{k=1}^{J} \hat{\pi}_k \hat{f}_k(x_0)} \quad \text{.................(2)}$$

$\hat{f}(X)$ – non-parametric estimated density function.
$\hat{\pi}$ – *a priori* class probability.
J – number of classes.

Adjusting Equation (2) for the calculation of each class, NP, SP and UP, Equation (3) is obtained:

$$\widehat{Pr}\left(G = Class \middle| X = x_0\right) = \frac{\hat{\pi}_{Class} \hat{f}_{Class}(x_0)}{\hat{\pi}_{Class} \hat{f}_{Class}(x_0) + \hat{\pi}_{notClass} \hat{f}_{notClass}(x_0)} \quad \text{....(3)}$$

Since each set of class and not-class is known, in order to eliminate any influence of an unbalancing of the sets, the *a priori* probability given any input x will be $\hat{\pi}_{Class} = 0.5$ and $\hat{\pi}_{notClass} = 0.5$. In this way, the *a posteriori* probability will be a result of the estimated probability density.

According to Equation (3), the *a posteriori* probability depends on the estimated densities with the class and not-class elements.

Thus, it is necessary to define a new variable Z, described in Equation (4):

$$Z = U_l - \max\left(U_m, U_n\right) \quad \text{.............................(4)}$$

such that l, m and n are the neurons of the output layer if, and only if, $l \neq m \neq n$.

Using the neural classifier developed for the elements that belong to the class, the values of Z will be greater than zero (true positive) when properly classified and negative when wrongly classified (false negative). For the elements that do not belong to the class, the values of Z will be negative when properly classified (true negative) and greater than zero when classified as the class (false positive). Table 3 presents the equation used in each class; a similar approach is presented in Silva[11].

Table 3. *Z* equations for the respective classes

Class	Class elements set	Sum of the two sets that do not belong to the class
NP	$Z_{NP} = U_1 - \max(U_2, U_3)$	$Z_{notNP} = U_1 - \max(U_2, U_3)$
SP	$Z_{SP} = U_2 - \max(U_1, U_3)$	$Z_{notSP} = U_2 - \max(U_1, U_3)$
UP	$Z_{UP} = U_3 - \max(U_2, U_1)$	$Z_{notUP} = U_3 - \max(U_2, U_1)$

According to Hastie[8], when two probability density curves follow the form presented in Figure 5, generated from hypothetical data, the *a posteriori* probability graphic calculated using Equation (3) will have the smooth form presented in Figure 6.

Observing the curve in Figure 6, a great similarity to the form of the curves generated from hyperbolic tangents is noticed, thus, for *posteriori* probabilities found, a regression using this function is carried out. From this moment on, the class probability can be written as a function of time and of Z, according to Equation (5):

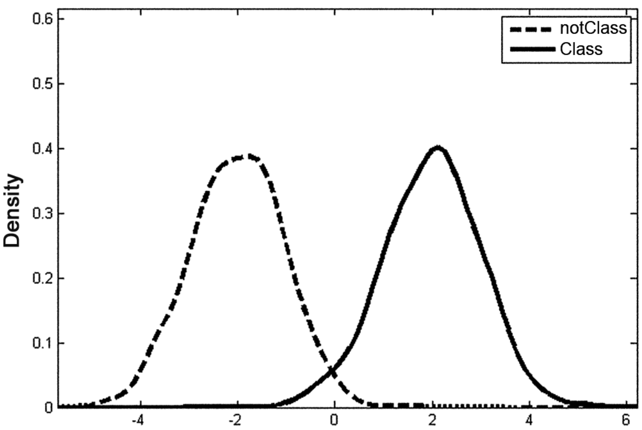

Figure 5. The continuous line represents the class probability density and the dashed line the density of the not-class. Hypothetical data

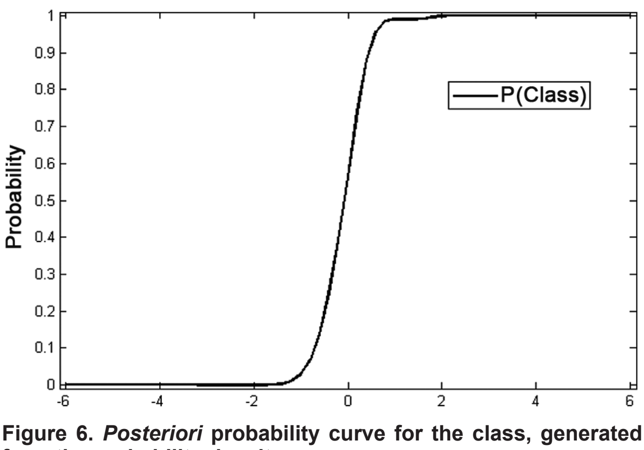

Figure 6. *Posteriori* probability curve for the class, generated from the probability density

$$P_{Class}\left(t\right) = a \times \tanh\left(b \times Z_n\left(t\right) - c\right) + d \quad \text{..................(5)}$$

4. Discussion and results

4.1 First testing

In order to sort the situation into three classes, the signals in Figure 7 were separated as NP class up to the time of 6868 s (181 bar), SP class (stable propagation) between 6869 s and 8143 s (208 bar) and UP class between 8144 s and 12,837 s (233 bar), resulting in 2207 samples being defined as NP, 1394 as SP and 6439 as UP. According to Pinto[2], the unbalance of data between the classes does not affect the performance of the trained network.

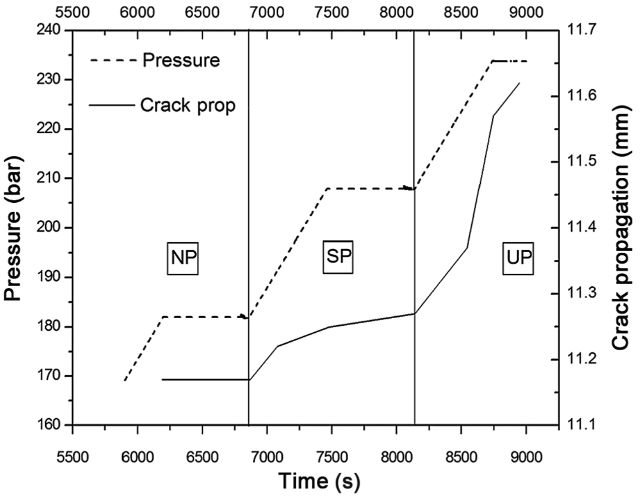

Figure 7. The dashed line represents the plot of pressure *versus* time and the continuous line represents the plot of crack propagation *versus* time

Initially, tests were made with the classification system considering the single positive value at the network output layer that the authors had already called 'without reclassification'. This methodology was presented by Silva *et al*[11].

In order to evaluate the quality of the neural network, two sets were tested: the first one was the same as that which had trained the network (training sets) and the second one was the data that was never shown to the network (test sets).

Table 4 shows that the performance of classification into three classes attained 78% for the training sets and 77% for the test sets, the nearness of results proving the generalisation of non-linear classifiers. It must be noted that the configuration of the neural network was the same in all the situations, as explained above.

Analysing separately the average rates of success of each one of the three classes studied, UP was the class that had the best performance at 92%, which was expected, since when there is unstable propagation of the defect, the acoustic emission events become more noticeable in the acquisition system. The SP class reached 77%, which proves that finding the exact moment of transition from no propagation of the defect to elastic propagation, and then the transition from elastic to plastic, is considerably more complex. The 'not classified' values (more than one positive output or all negative[11]) were expected because they usually occur in pattern recognition.

4.2 Second testing

As described in Section 2.4, the signals were divided into NP class, SP class and UP class, resulting in 2053 samples being defined as NP, 1045 samples as SP and 383 samples as UP.

Table 5 shows that the performance of the classification into three classes attained 91% for both sets. Analysing each individual class, it is noted that the trained neural network could discriminate correctly the three classes, including the SP class, which obtained an accuracy increase of about 10% when compared to the results

Table 4. Results of the average accuracy of 10 training and test sets (three classes without reclassification)

	Performance (training set)					Performance (test set)			
	NP	SP	UP	NC		NP	SP	UP	NC
NP	83%	4%	13%	12%	NP	82%	4%	14%	12%
SP	16%	77%	7%		SP	15%	77%	8%	
UP	4%	4%	92%		UP	4%	4%	92%	
Average total success	78%				Average total success	77%			
NC – not classified									

Table 5. Results of the average accuracy for 10 training and test sets (three classes without reclassification)

	Performance (training set)					Performance (test set)			
	NP	SP	UP	NC		NP	SP	UP	NC
NP	92.2%	6.4%	0.3%	0.3%	NP	93%	6.1%	0.3%	0.3%
SP	9.7%	86.7%	4.0%		SP	8.9%	84%	4.2%	
UP	0.7%	3.8%	95.4%		UP	1.4%	7.6%	91.4%	
Average total success	91%				Average total success	91%			
NC – not classified									

of the first test. The 'not classified' values (more than one positive output or all negative) were insignificant at almost zero.

4.3 POP curve

This section presents the results obtained for each class when applying the proposed method. The first POP curve is generated from the data obtained in test 2 and the second one from the data obtained in test 1.

Table 6 presents the regression function calculated from Equation (5) for each class. Through these functions, the probability that the input signal belongs to each class NP, SP and UP can be calculated.

Table 6. Hyperbolic tangent regression equations

Class	Equation	
NP	$P_{NP}(t) = 0.4951 \times \tanh(3.507 \times Z_{NP}(t) - 1.372) + 0.4999$	(6)
SP	$P_{SP}(t) = 0.4951 \times \tanh(0.7004 \times Z_{SP}(t) + 0.4588) + 0.4940$	(7)
UP	$P_{UP}(t) = 0.4745 \times \tanh(1.811 \times Z_{UP}(t) + 3.114) + 0.4925$	(8)

Figure 8 presents the probability of the NP class as a function of time; each dot represents the probability for each Z value, found by using Equation (6). As initially expected, the greater concentration of dots is next to one. Then, with the increase in test time, the greater concentration of dots is found close to zero.

The SP probability curve, Figure 9, initially presented the biggest value concentration close to zero. As time passed, the greater concentration turned to one, and as time increased the probability dropped again. This trajectory can be best visualised using the regression curve.

The UP probability is presented in Figure 10. As expected, it starts with an initial value concentration close to zero and, as it reaches 8000 s, the values start to concentrate close to one and remain equal to this value until the end of the testing.

Finally, the POP curve could be determined by plotting the three probability regression curves in one single graphic, as shown in Figure 11.

Since the curve was built from the dataset of test 2, it is known that until 6000 s the data is NP, from 6000 s to 8000 s it is SP and from 8000 s on it is UP.

Analysing the POP curve until 6000 s, as shown in Figure 12, the input signal possesses a greater probability of being characterised as NP until about 6000 s. When it reaches 5875 s, the probability of being classified as SP exceeds the NP probability.

Figure 13 highlights the SP data. For 6000 s, the probability for the signal to be classified as SP is the greatest among the three classes. From 6850 s on, the probability of SP starts dropping and that of UP starts rising. As it reaches 7640 s, the probability of UP exceeds SP.

Figure 14 highlights UP data. As the test time reaches 8000 s, the probability of the input signal being classified as UP is over 90%, while that of SP is approximately 10% and that of NP is almost zero.

To ratify the reproducibility of the method, the same procedure was applied to a different test, test 1.

Table 7 presents the equations used to find the probability for each value of Z and the POP curve obtained from these values is presented in Figure 15. According to what is described in Section 4.1, until 6870 s the input signal is classified as NP, from 6870 s to 8144 s as SP and from 8144 s on the classification is of UP.

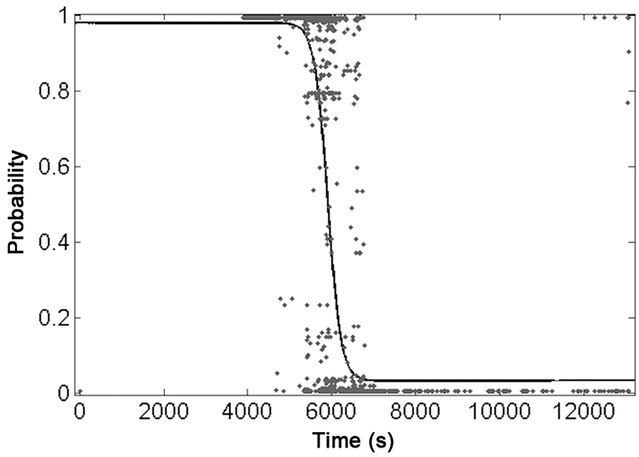

Figure 8. Probability of the NP class. The dots represent the probability for each value of *Z* and the continuous line is the regression function of these dots

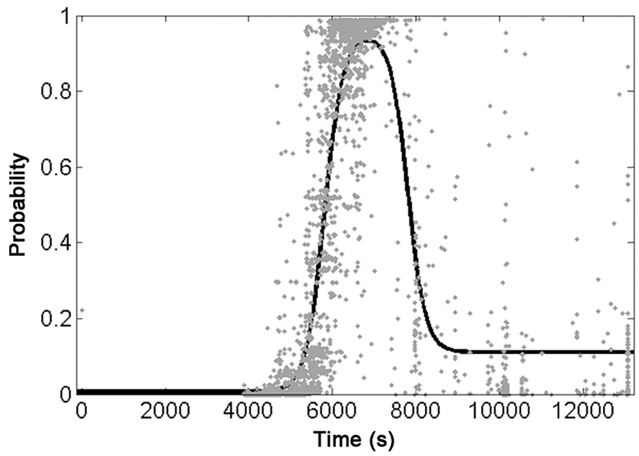

Figure 9. Probability of the SP class. The dots represent the probability for each value of *Z* and the continuous line is the regression function of these dots

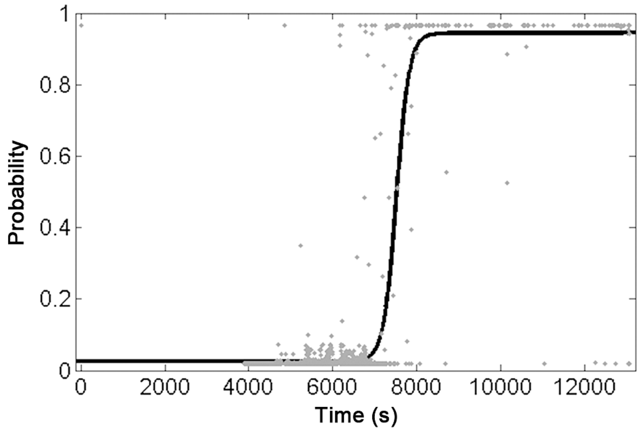

Figure 10. Probability for the UP class. The dots represent the probability for each value of *Z* and the continuous line is the regression function of these dots

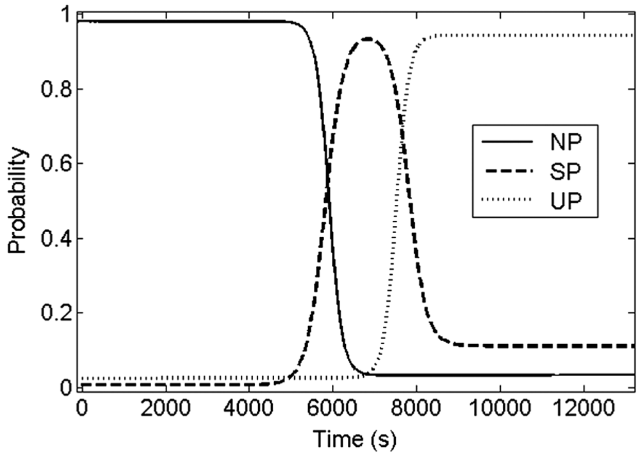

Figure 11. POP curve

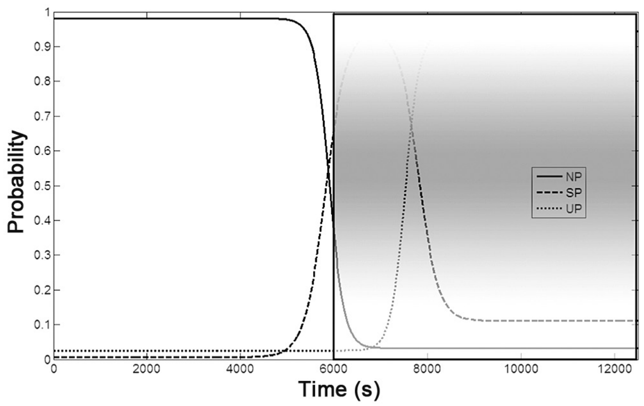

Figure 12. POP curve – highlighting NP data

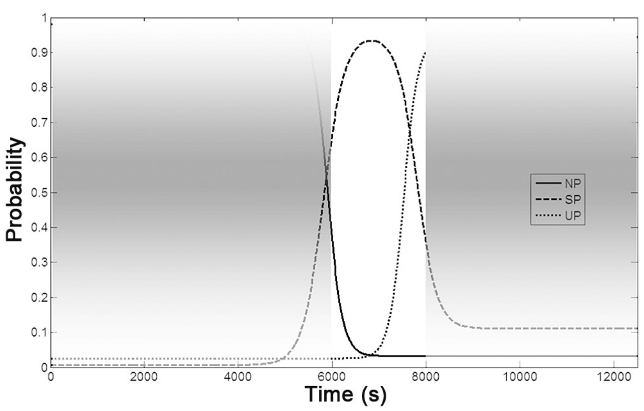

Figure 13. POP curve – highlighting SP data

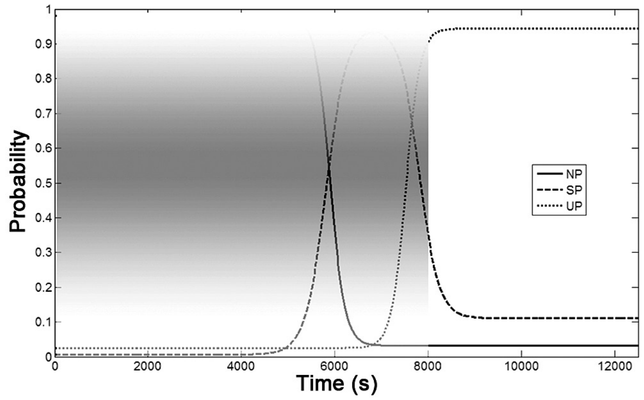

Figure 14. POP curve – highlighting UP data

Table 7. Hyperbolic tangent regression equations of test 1

Class	Equation	
NP	$P_{NP}(t) = 0.4764 \times \tanh(0.9566 \times Z_{NP}(t) + 0.788) + 0.4984$	(9)
SP	$P_{SP}(t) = 0.4541 \times \tanh(0.6761 \times Z_{SP}(t) + 0.6295) + 0.5584$	(10)
UP	$P_{UP}(t) = 0.4657 \times \tanh(0.653 \times Z_{UP}(t) - 0.5569) + 0.5229$	(11)

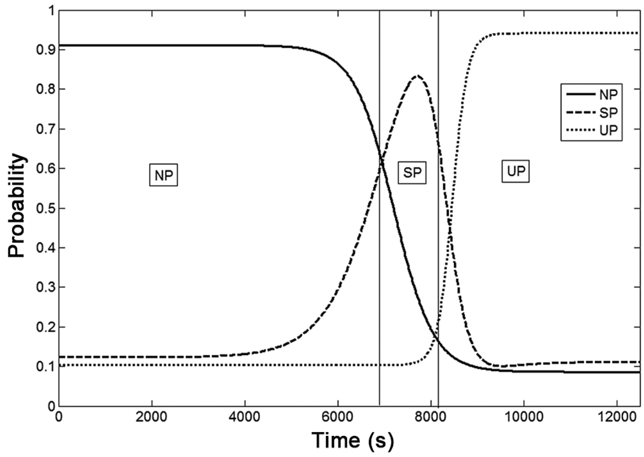

Figure 15. POP curve for test 1 – separated classes

Analysing Figure 15, it is observed, as expected, that the NP class possesses a greater probability value at the beginning of the test, being exceeded by the probability of SP at 6957 s, 87 s after the transition from NP to SP. While the NP class remains stable at 0.1 in the transition from SP to UP, the chance of a signal belonging to SP is even higher, but is already declining while the UP signal probability rises. The UP probability exceeds the SP value at 8414 s, that is with a delay of 270 s.

Defining the delays as classification errors, we have $ERROR_{NP/SP}$ as the ratio of the delay of the transition of NP to SP by total test time, and $ERROR_{SP/UP}$ as the ratio transition delay of SP to UP by total test time, according to Table 8. The errors presented show that the class transition presented by the POP curve is really close to the known real transition.

Table 8. Percentage classification error table

$ERROR_{NP/SP}$	2.1%
$ERROR_{SP/UP}$	0.68%

As a final discussion, it is highlighted that the crucial propagation moment is located at the threshold between the SP and UP classes, since the desired outcome is to predict, with a minimum advance, the beginning of an unstable defect propagation regime (or plastic propagation as denominated in fracture mechanics). Through the POP curves obtained so far, it has been proven that this technique is promising in this forecasting, it being possible to transform the pattern classifiers of the neural networks in bases for the development of an automatic crack propagation monitoring system in this equipment.

5. Conclusion

The paper presents an innovative methodology to identify, in an automatic way, the transition from stable to unstable crack propagation in rigid pressurised pipes, monitored by acoustic emission tests.

This project aimed to conduct a series of investigations for the separation of classes of acoustic emission signals for the monitoring of rigid ducts, building on previous studies[1,12]. Until now, studies have been focused mainly on trying to discriminate the classes, stable propagation (SP) from unstable propagation (UP).

In this project, we innovatively used classification into three classes and we attained approximately 91% of classification accuracy from the beginning of crack propagation until total breaking of the specimen, a rate considered significant in terms of the few features applied. However, the separation between NP and SP is far more complex than that between both NP and UP and SP and UP. This fact can be explained by the little difference that there is in terms of acoustic emission phenomena between the time of elastic deformation and the beginning of plastic deformation.

The proposed methodology of POP curves proved to be efficient, since in both tests studied so far, for the construction of curves, a similar behaviour and a form close to the proposed theoretical curve were obtained.

In relation to the method accuracy, the results obtained are very promising, since although the transition limits between the classes did not match the curve intersection points, which is the ideal situation, both were really close, presenting an irrelevant error when compared to the total test time.

Even though initial, there being much to be developed, such results show the capacity of classifying the propagation of cracks in rigid pipelines in a probabilistic way. It is a pioneer study, thus there are no previous references with which to compare the results.

It is important to emphasise that we are not aware of similar studies, to date, with the approach developed in the area of acoustic emission monitoring of the propagation of defects, so we could not compare our results.

6. Further studies

Further studies will involve applying the data of a test in another one to observe the behaviour of the curve and the accuracy of the method and adjusting the parameters used to obtain regression curves so that the intersections of the probability curves are closer to the moment of class transition.

A new three-year project is starting, aiming at performing four new tests, this time using test specimens of 25 m in length to be nearer to real field situations. The resulting AE signals will be used to repeat the methodology presented and to optimise the behaviour of the curves.

Acknowledgements

The authors would like to express their gratitude to CNPq, CAPES and FAPERJ for the financial support, the Signal Processing Laboratory at COPPE (LPS) for allowing the use of its computers and software, Petrobras for its cooperation and also the Federal University of Rio Grande do Sul.

References

1. R R Silva, S D Soares, L P Calôba, M H S Siqueira and J M A Rebello, 'Detection of the propagation of defects in pressurised pipes by means of the acoustic emission technique using artificial neural networks', Insight, 48 (1), pp 45-51, 2006.
2. C F C Pinto, 'Monitoração de Defeitos em Dutos Rígidos por Emissão Acústica e Redes Neurais', MSc dissertation, Universidade Federal do Rio de Janeiro, Rio de Janeiro, Brazil, 2011.
3. S Haykin, Neural Networks – A Comprehensive Foundation, Macmillan College Publishing Inc, USA, 1994.
4. R O Duda, P E Hart and D G Stork, Pattern Classification, 2nd Edition, USA, 2001.
5. R R Silva, M H S Siqueira, H S Marcio, M P V Souza, J M A Rebello and L P Calôba, 'Estimated accuracy of classification of defects detected in welded joints by radiographic tests', NDT&E International, 38, pp 335-343, 2005.
6. R R Silva, 'Reconhecimento de Padrões de Defeitos de Soldagem em Radiografias Industriais', DSc thesis, Universidade Federal do Rio de Janeiro, Rio de Janeiro, Brazil, 2003.
7. K Fukunaga, Introduction to Statistical Pattern Recognition, 2nd Edition, USA, 1990.
8. T Hastie, R Tibshirani and J Friedman, The Elements of Statistical Learning – Data Mining, Inference, and Prediction, 2nd Edition, USA, 2008.
9. D F Specht, 'Probabilistic neural network', Neural Network, Vol 3, pp 109-118, 1990.
10. Drleft, 'Comparison of a histogram and a kernel density estimate', site: http://en.wikipedia.org/wiki/File:Comparison_of_1D_histogram_and_KDE.png, 2010, em 23/04/2012.
11. R R Silva, L P Calôba, M H S Siqueira, L V S Sagrilo and J M A Rebello, 'Evaluation of the relevant characteristic parameters of welding defects and probability of correct classification using linear classifiers', Insight, 44 (10), pp 616-622, 2002.
12. R R Silva, D Mery and S D Soares, 'Evaluation of acoustic emission signal parameters for identifying the propagation of defects in pressurised tubes', Materials Evaluation, Vol 66, pp 493-500, 2008.
13. S D Soares, 'Correlações entre Emissão Acústica de Defeitos e Parâmetros de Mecânica da Fratura na Avaliação da Integridade de Equipamentos Pressurizados', DSc thesis, Universidade Federal do Rio de Janeiro, Rio de Janeiro, Brazil, 2008.